

New neutrino physics and the altered shapes of solar neutrino spectra

Ilídio Lopes*

*Centro Multidisciplinar de Astrofísica, Instituto Superior Técnico,
Universidade de Lisboa, Av. Rovisco Pais, 1049-001 Lisboa, Portugal*

Neutrinos coming from the Sun's core are now measured with a high precision, and fundamental neutrino oscillations parameters are determined with a good accuracy. In this work, we estimate the impact that a new neutrino physics model, the so-called generalized Mikheyev-Smirnov-Wolfenstein (MSW) oscillation mechanism, has on the shape of some of leading solar neutrino spectra, some of which will be partially tested by the next generation of solar neutrino experiments. In these calculations, we use a high-precision standard solar model in good agreement with helioseismology data. We found that the neutrino spectra of the different solar nuclear reactions of the proton-proton chains and carbon-nitrogen-oxygen cycle have quite distinct sensitivities to the new neutrino physics. The HeP and 8B neutrino spectra are the ones for which their shapes are more affected when neutrinos interact with quarks in addition to electrons. The shape of the ${}^{13}O$ and ${}^{17}F$ neutrino spectra are also modified, although in these cases the impact is much smaller. Finally, the impact in the shape of the PP and ${}^{13}N$ neutrino spectra is practically negligible.

I. INTRODUCTION

Since their discovery in 1956, neutrinos have always surprised physicists due to their unexpected properties, often challenging our basic understanding of the standard model of particle physics (in the remainder of the article, it will be called simply the 'standard model') and the properties of elementary particles. In particular, the discovery of neutrino flavour oscillations stands as one of the most convincing proofs that the standard model is incomplete as it does not explain all the known experimental properties of the fundamental particles.

The neutrino research success has been made possible mostly due to many dedicated experiments performed during the last fifty years. It is worth highlighting the contributions of some pioneering experiments, among others, such as the Super-Kamiokande detector [1, 2] where the oscillation of atmospheric neutrinos was discovered, and the SNO detector [3] where the fluxes of all neutrino flavour species produced in the Sun's core were measured for the first time. Many other experiments done during the previous decades have contributed for the success of this story, in particular, the solar neutrino experiments. Despite their technical complexities, these experiments were able to measure the electron neutrino fluxes coming from the Sun and played a major role in the establishment of the so-called solar neutrino problem – a discrepancy between the theoretical prediction of neutrino fluxes and their experimental measurements: the experimental value being one third of the predicted value. This fact was evidenced for the first time by the Homestake Experiment of Ray Davis [4], and confirmed by many other experiments that followed. It was the solar neutrino problem that prompted the development of the neutrino flavour oscillation model.

If indeed the previous generation of solar neutrino detectors has been one of the beacons of particle physics, both by leading the way in uncovering the basic properties of particles, including the nature of neutrino flavour oscillations, and

by being responsible for developing pioneering techniques in experimental neutrino detection [5], the next generation of detectors is equally promising in discovering new physics. Among various, some of which will be looking for evidence of neutrino new physics we can mention the following future detectors: the Low Energy Neutrino Astronomy [LENA, 6], the Jiangmen Underground Neutrino Observatory [JUNO, 7], the Deep Underground Neutrino Experiment [DUNE, 8], the NO ν A Neutrino Experiment [NO ν A, 9], and the Jinping Neutrino Experiment [Jinping, 10].

These detectors will measure with high precision the neutrino fluxes and neutrino spectra of a few key neutrino nuclear reactions, such as the 8B electron-neutrino (${}^8B\nu_e$) spectrum produced by the β -decay process in the 8B solar (chain) reaction: ${}^7Be(p, \gamma){}^8(e^+\nu_e){}^8B^*(\alpha){}^4He$ [11, 12]. This will allow us to probe in detail the Sun's core, including the search for new neutrino physics interaction or even new physics processes. Moreover, the high quality of the data will enable the development of inversion techniques for determining basic properties of the solar plasma [e.g., 13]. Specific examples can be found in Balantekin et al. [14] and Lopes [15]. Equally, solar neutrino data can be used to find specific features associated with possible new physical processes present in the Sun's interior [e.g. 16], such as the possibility of an isothermal solar core associated with the presence of dark matter [17].

Today, the basic principles of neutrino physics are firmly established, neutrinos are massive particles with a lepton flavours mix. The parameters describing neutrino flavour oscillations are measured with great accuracy and precision, which has been possible due to the extensive studies made by many different types of neutrino experiments: solar and atmospheric neutrino observatories, nuclear reactors and experimental particle accelerators [e.g., 18–20]. Section III C presents the status of the current neutrino oscillation parameters obtained from up-to-date experimental data.

Even if many properties of neutrinos are known, many others are still a mystery:

- firstly, are neutrinos Majorana or Dirac fermions ? i.e., are neutrinos their own anti-particle ? Although the theoretical expectation favours the first option, only experimental ev-

* ilidio.lopes@tecnico.ulisboa.pt

idence can settle this question;

- secondly, what is the mass hierarchy of neutrinos ? In other words, does the order of neutrino masses between the different particle families follow a *normal hierarchy* – two light neutrinos followed by a heavier one, or an *inverted hierarchy* – one light neutrino follow by two heavier ones ?

Together with the CP violation in the lepton sector, these are the most important questions of neutrino physics. Some of these questions will be answered by the next generation of neutrino experiments – the long baseline neutrino experiments and solar neutrino telescopes. Nevertheless, it is necessary to improve the current neutrino flavour model to take full advantage of the forthcoming experimental data.

Despite the success of the current neutrino physics model in explaining most of the neutrino’s known observed properties, the solution encountered clearly indicate the existence of new physics beyond the standard model. As such, this implies that within the current particle physics theoretical framework, experiments can study neutrinos in other types of interactions. When such processes occur, these lead to important modifications of the physical mechanisms by which neutrinos are created, propagate and interact with other particles of the standard model. This new class of neutrino interactions is usually known as non-standard interactions (*nsi*).

The non-standard interactions of neutrinos have been extensively studied in the literature, among others reviews on this topic, see for instance Miranda and Nunokawa [21], Ohlsson [22]. Moreover, the constraints on the *nsi* parameters and their effects for low energy neutrinos have been derived from a great variety of experimental results. Until now no definitive evidence of non-standard interactions has been provided by the experimental data. Actually, all observations made as yet can be explained in terms of the standard interactions of the three known neutrinos, although some of them need the help of sterile neutrinos. Nevertheless, in some cases the non-standard interactions of neutrinos provide an interesting and valid alternative [e.g., 23]

In this work we are mostly concerned with the non-standard interactions of solar neutrinos. These interactions can affect the neutrino production inside the Sun, the detection of neutrinos by experimental detectors and the neutrino propagation in the Earth’s and Sun’s interiors. In particular, our study focus on the propagation of neutrinos through baryonic matter in the Sun’s interior, a process usually known as the generalized Mikheyev-Smirnov-Wolfenstein (*MSW*) oscillation mechanism, or generalized matter effect oscillations. Our goal is to make predictions about the modifications imprinted by this new generalized *MSW* on the shape of the solar neutrino spectrum produced by some of the (pp) and carbon-nitrogen-oxygen (CNO) key nuclear reactions, like *HeP* and ^8B neutrino spectra.

The high quality of the standard solar model in reproducing the measured solar neutrino fluxes, and the observed acoustic frequency oscillations, make it a privileged tool to look for the new interactions within a generalized Mikheyev-Smirnov-Wolfenstein mechanism occurring in the Sun’s interior. The standard solar model [SSM, 24] partly validated by helioseis-

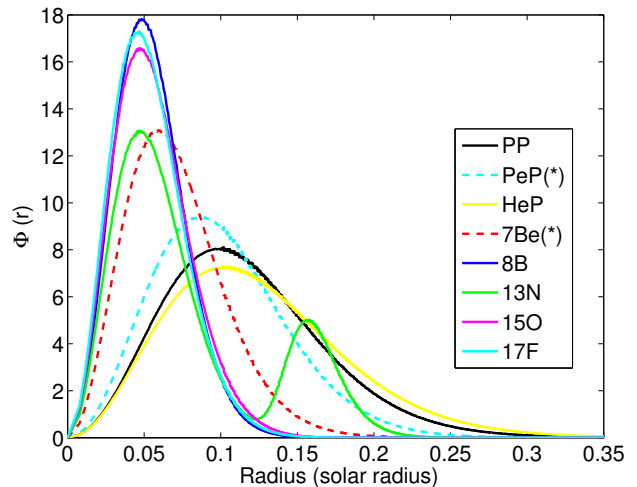


FIG. 1. The electron-neutrino fluxes produced in the various nuclear reactions of the pp chains and CNO cycle. These neutrino fluxes were calculated for a standard solar model using the most updated microscopic physics data. This solar model is in agreement with the most current helioseismology diagnostic and other solar standard models published in the literature (see text). For each neutrino type j (with $j = PP, PeP(*), HeP, ^8B, ^7Be(*), ^{13}N, ^{15}O, ^{17}F$), $\Phi_j(r) \equiv (1/F_j) df_j(r)/dr$ is drawn as a function of the fractional radius r for which f_j is the flux in s^{-1} and F_j is the total flux for this neutrino type. The neutrino sources noted with the symbol (*) correspond to spectral lines. The same colour scheme is used in figures 4 and 5.

mology, predicts that the density inside the Sun varies from about 150 g cm^{-3} in the centre of the star, to 1 g cm^{-3} at half of the solar radius. The variation of density of matter with the solar radius is followed by identical variations on the local quantities of electrons and quarks. Moreover, the different type of quarks will also be affected by the local distribution of chemical elements (most noticeably Hydrogen and Helium) which lead to a not obvious distribution of up- and down-quarks. Therefore, we can anticipate that the current standard solar model combined with data coming from the next generation of the solar neutrino detections, will allow us to put much stronger constraints in the non-standard interactions of neutrinos.

In the next section, we review the current status of the standard solar model and neutrino production in the Sun’s core, In Section III, we present a summarised discussion about the current standard neutrino oscillation flavour model, and a generalized model for which neutrinos have new types of interactions with standard particles. In Section IV, we compute the neutrino spectra resulting from these new types of interactions. In the final section we discuss the results and their implications for the future neutrino experiments.

II. NEUTRINO PRODUCTION IN THE SUN'S CORE

A. Helioseismology and the standard solar model

During the last three decades helioseismology has provided solar physics with a tool that describes with unprecedented quality the internal structure of the Sun from its surface up to the deepest layers of the Sun's interior. This has allowed astronomers to characterise with great precision the different solar neutrino sources. Equally, this discipline has stimulated the development of inversion techniques to probe the internal solar dynamics. Today an impressive agreement has been reached between the neutrino flux predictions and the neutrino flux measurements made by the existing neutrino detectors. The high quality of the helioseismology data has allowed to compute an exceptionally accurate model of the Sun's interior - the standard solar model. The neutrino fluxes predictions of the solar model have an accuracy comparable to the current measurements made by particle accelerators or nuclear reactors.

The standard solar model in this study is obtained using a version of the one-dimensional stellar evolution code CE-SAM [25]. The code has an up-to-date and very refined microscopic physics (updated equation of state, opacities, nuclear reactions rates, and an accurate treatment of the microscopic diffusion of heavy elements), including the solar mixture of Asplund et al. [26, 27]. This solar model is calibrated to reproduce with high accuracy the present total radius, luminosity and mass of the Sun at the present $t_{\odot} = 4.54 \pm 0.04$ Gyr [28]. Moreover, this model is required to have a fixed value of the photospheric ratio $(Z/X)_{\odot}$, where X and Z are the mass fraction of hydrogen and the mass fraction of elements heavier than helium. This solar standard model shows acoustic seismic diagnostics and solar neutrino fluxes similar to other models found in the literature [24, 29–34]

This solar model is calibrated for the present day solar data with a high accuracy. Therefore slightly different physical assumptions, will lead to different radial profiles of temperature, density and chemical composition, among other quantities. These changes result from readjustments of the Sun's internal structure caused by the need to obtain the same total luminosity. In particular, the neutrino fluxes and sound speed profile will be very sensitive to the radial distributions of the previous quantities. As such, using the high precision data from helioseismology, it is possible to put strong constraints to the internal structure of the Sun and its neutrino fluxes [28, 35].

The current uncertainty between the square of the sound speed profile inferred from helioseismology acoustic data and the one obtained from the standard solar model using the up-to-date photospheric abundances Asplund et al. [27] is smaller than 3% for any layer of the Sun's interior. Although there is a difference between the sound speed profile computed using an older mixture of abundances by Grevesse and Sauval [36] or the new mixture of Asplund et al. [27], for this study these effects are negligible on the radial variation of electrons, protons and neutrons. This is even more so, since recent measurements of the solar metallicity abundances suggest that the

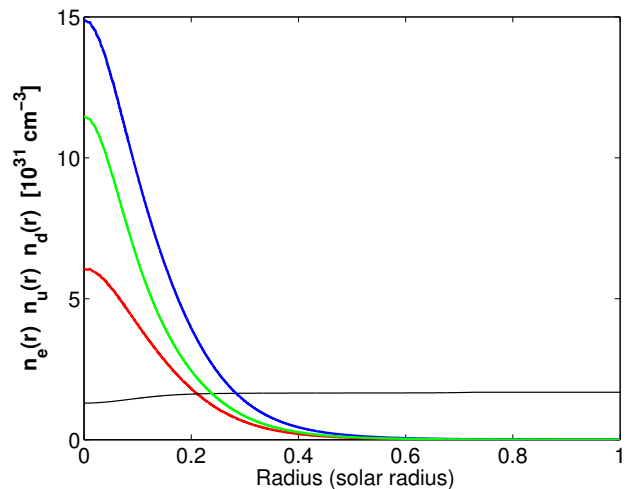


FIG. 2. The solar plasma is constituted mostly by electrons, protons and neutrons. Variation of the number density of electrons $n_e(r)$ (red curve), up-quarks $n_u(r)$ (blue curve) and down-quarks $n_d(r)$ (green curve), and the relative variation of up and down quarks $n_u(r)/n_d(r)$ (black curve). In the center $n_u/n_d = 1.3$ and near the surface $n_u/n_d = 1.7$.

sound speed difference of helioseismic data and standard solar model is reduced further [37].

Particularly relevant for our study is the radial profile of the electron, proton and neutron densities inside the Sun, since these quantities are fundamental ingredients to test the non-standard neutrino physics theories.

B. The solar neutrino sources

The neutrino fluxes produced in the nuclear reactions of the pp chains and CNO cycle have been computed for an updated version of the solar standard model, as discussed in the previous section. Figure 1 shows the location of the different neutrino emission regions of the nuclear reactions for an up-to-date SSM. In the Sun's core, the neutrino emission regions occur in a sequence of shells, following closely the location of nuclear reactions, orderly arranged in a sequence dependent on their temperature. The helioseismology data and solar neutrino fluxes guaranties that such neutrino shells are known with a great accuracy. The leading source of the energy in the present Sun are the pp chains nuclear reactions, since the CNO cycle nuclear reactions contribute with less than 2%. The first reaction of the pp chains is the $PP-\nu$ reaction which has the largest neutrino emission shell, a region that extends from the centre to $0.30 R_{\odot}$. The $PeP-\nu$ reaction has a neutrino emission shell which is similar to the PP reaction, but with a shell of $0.25 R_{\odot}$. These nuclear reactions are strongly dependent on the total luminosity of the star. Alternatively, the neutrino emission shells of ${}^8B-\nu$ and ${}^7Be-\nu$ extend up to $0.15 R_{\odot}$ and $0.22 R_{\odot}$. It is interesting to notice that the maximum emission of neutrinos for the pp chains nuclear reactions, follows an ordered sequence (see figure 1): ${}^8B-\nu$, ${}^7Be-\nu$, $PeP-\nu$ and $PP-$

ν with the maximum emission located at 0.05, 0.06, 0.08 and 0.10 R_\odot . The known neutrino emission shells of the different CNO cycle nuclear reactions are the following ones: $^{15}\text{O}-\nu$, $^{17}\text{F}-\nu$ and $^{13}\text{N}-\nu$. These shells are similar to the $^8\text{B}-\nu$ emission shell. The $^{13}\text{N}-\nu$ have two independent shells: one in the Sun's deepest layers of the core and a second shell located between 0.12 and 0.25 of R_\odot . The emission of neutrinos for $^{15}\text{O}-\nu$, $^{17}\text{F}-\nu$ and $^{13}\text{N}-\nu$ shells is maximal at 0.04 - 0.05 of R_\odot . The $^{13}\text{N}-\nu$ neutrinos have a second emission maximum which is located at 0.16 R_\odot .

C. Neutrinos, Electrons and Quarks

The electron density $n_e(r) = N_o \rho(r)/\mu_e(r)$ where μ_e is the mean molecular weight per electron, $\rho(r)$ the density of matter and N_o the Avogadro's number. In this model we will consider the impact on the quarks up and down. Accordingly, the density of up and down quarks will be computed from a relation analogous to $n_e(r)$, $n_i(r) = N_o \rho(r)/\mu_i(r)$ (with $i = u, d$) where $\mu_i(r)$ is the mean molecular weight per quark given by

$$\mu_i(r) = \left[(1 + \delta_{iu})X(r) + \frac{3}{2}Y(r) + \frac{3}{2}Z(r) \right]^{-1} \quad (1)$$

where $i = u, d$ with $X + Y + Z = 1$. The distribution of electrons and up and down quarks, as a function of the radius of the Sun for the standard solar model, is shown in figure 2. The mean molecular weight per quark is dominated by Hydrogen and Helium since the only other elements included in Z like Carbon, Nitrogen, Oxygen and heavier elements contribute with a very small fraction to the solar plasma. Although the Z -variation can affect the evolution of the star in the way it affects the radiative transport [37], its impact on the si and nsi MSW interactions for $\mu_i(r)$, $i = u, d$ is small since the relative radial variation between up- and down-quarks due to Z -variation is not significant.

III. MODEL OF NEUTRINO PHYSICS OSCILLATIONS

A. basic neutrino physics

In the Standard Model, neutrinos interact with other particles only via weak standard interactions (si), which are described by the Lagrangian \mathcal{L}_{si} which can be decomposed into components describing the charged and neutral interactions [38–40]. Nevertheless, in the current study, we choose to write the Lagrangian \mathcal{L}_{si} as an effective interaction Lagrangian [40, 41], which at low and intermediate neutrino energies reads

$$\mathcal{L}_{si} = -2\sqrt{2}G_F g_p^f (\bar{\nu}_\alpha \gamma_\rho L \nu_\alpha) (\bar{f} \gamma^\rho P f) \quad (2)$$

where f denotes a lepton or a quark, such as the u -quark and the d -quark, ν_α are the three light neutrinos (with the subscript $\alpha = e, \mu, \tau$), P is the chiral projector (is equal to R or L such that $R, L \equiv (1 \pm \gamma^5)/2$) and g_p^f denotes

the strength of the interaction (ns) as defined in the standard model between neutrinos of flavours α and β and the P -handed component of the fermion f . Specifically, the g_p^f coupling (left- and right- handed coupling, i.e., g_L^f and g_R^f) for the u -quark (and c - and t -quark) to the Z -boson corresponds to $g_L^u = 1/2 - 2/3 \sin^2 \theta_w$ and $g_R^u = -2/3 \sin^2 \theta_w$. Similarly, the g_p^f for the d -quark (and s - and b -quark) corresponds to $g_L^d = -1/2 + 1/3 \sin^2 \theta_w$ and $g_R^d = 1/3 \sin^2 \theta_w$, the g_p^f for the electron corresponds to $g_L^e = -1/2 + \sin^2 \theta_w$ and $g_R^e = \sin^2 \theta_w$ and the g_p^f for the neutrino (ν_α with $\alpha = e, \mu, \tau$) corresponds to $g_L^\nu = 1/2$ and $g_R^\nu = 0$. θ_w is the Weinberg mixing angle [42, 43], with a typical value of $\sin^2 \theta_w \approx 0.23$ [44].

The evolution of a generic neutrino state $\nu_\alpha \equiv (\nu_e \nu_\mu \nu_\tau)^T$ is described by a Schrödinger-like equation [38], that expresses the evolution of the neutrino between the flavour states [38] with the distance r , from neutrinos that are produced in the Sun's core until their arrival to the Earth's neutrino detectors. The equation reads

$$i \frac{d\nu_\alpha}{dr} = \mathcal{H}\nu_\alpha = (\mathcal{H}_v + \mathcal{H}_m)\nu_\alpha, \quad (3)$$

where \mathcal{H} is the total Hamiltonian, \mathcal{H}_v and \mathcal{H}_m are the Hamiltonian components expressions for vacuum and in matter flavour variations, such that $\mathcal{H}_v \equiv M_\nu^\dagger M_\nu / 2p_\nu$ where M_ν is the mass matrix of neutrinos (the term proportional to the neutrino momentum p_ν is omitted here), and \mathcal{H}_m is the Hamiltonian (a diagonal matrix of effective potentials) which depends on the properties of the solar plasma, i.e., the density and composition of the matter, such that $\mathcal{H}_m = \text{diag}(V_e, V_\mu, V_\tau)$.

The flavour evolution is described in terms of the instantaneous eigenstates of the Hamiltonian in matter $\nu_m \equiv (\nu_{1m}, \nu_{2m}, \nu_{3m})^T$. These eigenstates are related to the flavour states by the mixing matrix in matter, U_m : $\nu_\alpha = U_m^m \nu_m$.

B. The effective matter potential

As neutrinos propagate in the Sun's interior, they will oscillate between the three flavour states ν_e, ν_μ and ν_τ due to vacuum oscillations, however in the highly dense medium which is the Sun's interior, contrary to their propagation in vacuum, the scattering of neutrinos with other elementary particles, like electrons, will enhance their oscillation between flavour states. Indeed, neutrinos propagating in a dense medium like the Sun (or Earth) have their flavour between states affected by the coherent forward scattering, i.e., coherent interactions of the neutrinos with the medium background [38]. The interaction of neutrinos with the medium proceeds through coherent forward elastic Charged-Current (cc) and Neutral-Current (nc) scatterings, which as usual are represented by the effective potentials V_α^{cc} and V_α^{nc} for each of the three type of neutrinos.

Therefore, at low energies, the potentials can be evaluated by taking the average of the effective four-fermion Hamiltonian due to exchange of W and Z bosons over the state describing the background medium. Accordingly, for a non-

relativistic un-polarized medium, for the effective potential of ν_e, ν_μ and ν_τ neutrinos, one obtains

$$V_\alpha = V_\alpha^{cc} + V_\alpha^{nc}, \quad (4)$$

where $\alpha = e, \mu, \tau$.

Let us consider that the solar internal medium is mainly composed of electrons, up-quarks and down-quarks as in protons and neutrons with the corresponding $n_e(r)$, $n_u(r)$ and $n_d(r)$ local number densities. The contribution to \mathcal{H}_m due to the cc scattering of electron neutrinos ν_e (produced in the Sun's core) propagating in a homogeneous and isotropic gas of unpolarized electrons (like the electron plasma found in the Sun's interior) is given by

$$V_e^{cc} = \sqrt{2}G_F n_e(r) \quad (5)$$

where G_f is the Fermi constant. For ν_μ and ν_τ , the potential due to its cc interactions is zero for most of the solar interior since neither μ 's nor τ 's are present, therefore,

$$V_\mu^{cc} = V_\tau^{cc} = 0 \quad (6)$$

Generically, for any active neutrino, the V_α^{cc} reads

$$V_\alpha^{cc} = \delta_{\alpha e} \sqrt{2}G_F n_e(r) \quad (7)$$

Analogously, one determines V_α^{nc} for any neutrino due to nc interactions. Since nc interactions are flavour independent, these contributions are the same for neutrinos of all three flavours. The neutral-current (nc) potential reads

$$V_\alpha^{nc} = \sum_f \sqrt{2}G_F g_v^f n_f(r) \quad (8)$$

where $\alpha = e, \mu, \tau$ and $f = e, u, d$. $n_f(r)$ is number density of fermions, electrons, up-quarks (u) and down-quarks (d) as in protons (uud) and neutrons (udd). The factors g_v^f are the axial coupling to fermions ($g_v^e = -1/2 + 2\sin^2\theta_w$, $g_v^u = 1/2 - 4/3\sin^2\theta_w$ and $g_v^d = -1/2 + 2/3\sin^2\theta_w$, see for example Giunti and Chung [45]). Therefore the effective potential [38] for any active neutrino due to the neutral-current V_α^{nc} reads

$$V_\alpha^{nc} = \sqrt{2}G_F [g_v^e n_e(r) + g_v^u n_u(r) + g_v^d n_d(r)]. \quad (9)$$

where $n_u(r)$ and $n_d(r)$ are the analogue of $n_e(r)$, i.e., the number density of up-quarks and down-quarks in the Sun's interior.

Using equations (7) and (8) in equation (4), the effective potential for any active neutrino crossing the solar plasma reads

$$V_\alpha = \sqrt{2}G_F [\delta_{\alpha e} n_e + g_v^e n_e + g_v^u n_u + g_v^d n_d]. \quad (10)$$

When neutrinos propagate through matter, the forward scattering of neutrinos off the background matter will induce an index of refraction for neutrinos. This is the exact analogous to the index of refraction of light travelling through matter. However, the neutrino index of refraction will depend on the neutrino flavour, as the background matter contains different amounts of scatters for the different neutrinos flavours.

The effective potentials V_α are due to the coherent interactions of active flavour neutrinos with the medium through coherent forward elastic weak cc and nc scatterings.

Inside the Sun, as local matter is composed of neutrons, protons, and electrons, the effective potential V_α for the different neutrino species (including ν_e neutrinos) has a quite distinct form which depends on the local number densities $n_e(r)$, $n_u(r)$ and $n_d(r)$, quantities which depend on the chemical composition (its metallicity Z) of the Sun's interior. Nevertheless, at first approximation, since electrical neutrality implies locally an equal number density of protons (uud) and electrons, V_α takes a more simple form (equation 10), as the nc potential contribution of protons and electrons cancel each other. Therefore, only neutrons (udd) contribute to V_α^{nc} . Hence the last two terms of equation (9) can be expressed as $g_v^n n_n(r)$ to only take into account the quark contribution for neutrons. In this expression $n_n(r)$ is the local density of neutrons and the g_v^n is the neutron coupling constant, it follows that $g_v^n = g_v^u + 2g_v^d = -1/2$, and equation (9) reads $V_\alpha^{nc} = -\sqrt{2}/2G_F n_n(r)$. Now V_α (equation 10) inside the Sun yields

$$V_\alpha = \sqrt{2}G_F \left[\delta_{\alpha e} n_e(r) - \frac{1}{2} n_n(r) \right]. \quad (11)$$

where $\alpha = e, \mu, \tau$.

As we will discuss later, only effective potential differences affect the propagation of neutrinos in matter [46], accordingly, one defines the potential difference between two neutrino flavours α and β as

$$V_{\alpha\beta} = V_\alpha - V_\beta, \quad (12)$$

where $\alpha, \beta = e, \mu, \tau$.

The Sun's interior is a normal medium composed of nuclei (protons and neutrons) and electrons. Since the effective potential for muon and tau neutrinos, V_α (with $\alpha = \mu, \tau$ or a combination thereof) is due to the neutral current scattering only (see equation 11), this leads to $V_{\mu\tau} = V_\mu - V_\tau = 0$. However, as the effective potential for electron neutrinos depends on the neutral and charged current scatterings, in this case

$$V_{e\alpha} = \sqrt{2}G_F n_e(r), \quad (13)$$

where $\alpha = \mu, \tau$ or a combination thereof. Although for the Sun and Earth only charged current interactions with electrons are the only effective potential that contributes to the propagation of electron neutrinos, there are other types of non-typical matter, like the one found in the core of supernovae and in the early Universe for which the effective potential difference $V_{\alpha\beta}$ has a much stronger dependence on the properties of the background plasma [43, 46].

C. Neutrino oscillation data parameters

As shown in the previous section, the neutrino flavour oscillations model is described with the help of 6 mixing parameters all of which are determined from experimental data [47].

The quantities are the following ones: the difference of the squared neutrino masses Δm_{21}^2 , Δm_{31}^2 , the mixing angles $\sin^2 \theta_{12}$, $\sin^2 \theta_{13}$, $\sin^2 \theta_{23}$ and the CP-violation phase δ_{CP} .

The mass square differences and mixing angles are known with a good accuracy [48, 49]: Δm_{31}^2 is obtained from the experiments of atmospheric neutrinos and Δm_{12}^2 is obtained from solar neutrino experiments.

The mixing angles are not uniformly well defined: θ_{12} is obtained from solar neutrino experiments with an excellent precision; θ_{23} is obtained from the atmospheric neutrino experiments, this is the mixing angle of the highest value; θ_{13} has been firstly estimated from the Chooz reactor [50], its value is very small and was still very uncertain [51]. Nowadays with Daya Bay and Reno, the situation has largely improved [52]. However, present experiments cannot fix the value of the CP-violation phase [53].

An overall fit to the data obtained from the different neutrino experiments: solar neutrino detectors, accelerators, atmospheric neutrino detectors and nuclear reactor experiments suggests that the parameters of neutrino oscillations are the following ones [48, 49]: $\Delta m_{31}^2 \sim 2.457 \pm 0.045 \cdot 10^{-3} eV^2$ or $(\Delta m_{31}^2 \sim -2.449 \pm 0.048 \cdot 10^{-3} eV^2)$, $\Delta m_{21}^2 \sim 7.500 \pm 0.019 \cdot 10^{-5} eV^2$, $\sin^2 \theta_{12} = 0.304 \pm 0.013$, $\sin^2 \theta_{13} = 0.0218 \pm 0.001$, $\sin^2 \theta_{23} = 0.562 \pm 0.032$ and $\delta_{CP} = 2\pi/25 \cdot n$ with $n = 1, \dots, 25$.

In the limiting case where the value of the mass differences, Δm_{12}^2 or Δm_{31}^2 is large, or one of the angles of mixing ($\theta_{12}, \theta_{23}, \theta_{31}$) is small, the theory of three neutrino flavour oscillations reverts to an effective theory of two neutrino flavour oscillations [53]. Balantekin and Yuksel have shown that the survival probability of solar neutrinos calculated in a model with two neutrino flavour oscillations or three neutrino flavour oscillations have very close values [54].

D. The survival of electron neutrinos

Mostly motivated by solar neutrino data, the focus of this work is the study of the propagation of electron neutrinos, in particular to determine the survival probability of electron neutrinos P_e ($\equiv P(\nu_e \rightarrow \nu_e)$) arriving on Earth which have their flavour changed due to vacuum and solar matter oscillations. Luckily, in the Sun P_e takes a particularly simple form, since the evolution of neutrinos in matter is adiabatic and for that reason their contribution for P_e can be cast in a similar manner to the vacuum-oscillation expression. Accordingly, the standard parametrization of the neutrino mixing matrix leads to the following survival probability for electron neutrinos, P_e reads

$$P_e = c_{13}^2 c_{13}^{m2} P_2^{ad} + s_{13}^2 s_{13}^{m2} \quad (14)$$

where $c_{ij} = \cos \theta_{ij}$, $s_{ij} = \sin \theta_{ij}$, and P_2^{ad} reads

$$P_2^{ad} = \frac{1}{2} (1 + \cos(2\theta_{12}) \cos(2\theta_{12}^m)). \quad (15)$$

The matter angles, θ_{12}^m and θ_{13}^m which depends equally of the fundamental parameters of neutrino flavour oscillation and the properties of solar plasma are determined as follows:

- The mixing angle θ_{12}^m is determined by

$$\cos(2\theta_{12}^m) = -\frac{V_{12}^*}{\sqrt{V_{12}^{*2} + (A_{12}^{*-1} \sin(2\theta_{12}))^2}} \quad (16)$$

where the effective potential $V_{12}^*(E, r)$ reads

$$V_{12}^*(E, r) = c_{13}^2 - A_{12}^{*-1} \cos(2\theta_{12}) \quad (17)$$

where $A_{12}^* = A_*/\Delta m_{12}^2$ and $A_* = 2EV_{\alpha\beta}$ [38]. The parameter $A_*(E, r)$ contains the effect of matter on the electron neutrino propagation as defined by $V_{\alpha\beta}$, given by equation (13). In the specific case of electron neutrinos, $A_*(E, r) = 2E \sqrt{2}G_F n_e(r)$ (with $V_{e\alpha} = \sqrt{2}G_F n_e(r)$).

- The mixing angle θ_{13}^m , accordingly to Goswami and Smirnov [55], is determined by

$$\sin^2(\theta_{13}^m) \approx \sin^2(\theta_{13}) [1 + 2A_{13}^*] \quad (18)$$

with $A_{13}^* = 2EV_e^o/\Delta m_{31}^2$, where V_e^o is the effective potential at the electron neutrino production radius r_o , i.e., $V_e^o = \sqrt{2}G_F n_e(r_o)$. The value of r_o is different for the different neutrino sources of the pp chains and CNO cycle.

E. New Neutrino Physics

In the presence of physics beyond the standard model [e.g., 56], the neutral current interactions that are flavour diagonal and universal in the standard model can have a more general form. Hence, new interactions arise between neutrinos and matter, which conveniently one defines as non-standard interactions (*nsi*), these new neutrino interactions with fermions are described by a new effective lagrangian [e.g., 41, 57, 58]. Accordingly, the classical lagrangian (equation 2) is generalized to take into account these new types of interactions previously forbidden. The new lagrangian reads

$$\mathcal{L}_{nsi} = -2\sqrt{2}G_F \epsilon_{\alpha\beta}^{fP} (\bar{\nu}_\alpha \gamma_\rho L \nu_\beta) (\bar{f} \gamma^\rho P f) \quad (19)$$

where $\epsilon_{\alpha\beta}^{fP}$ is the equivalent of g_p^f for the standard interactions (equation 2), which corresponds to the parametrization of the strength of the non-standard interactions between neutrinos of flavours α and β and the P -handed component of the fermion f [e.g., 56]. Without loss of generality we consider only neutrino interactions with up- and down-quarks [e.g., 59]. In the latter Lagrangian, $\epsilon_{\alpha\beta}^{fP}$ corresponds to two classes of non-standard terms: flavour preserving non-standard terms proportional to $\epsilon_{\alpha\alpha}^{fP}$ (known as non-universal interactions), and flavour changing terms proportional to $\epsilon_{\alpha\alpha}^{fP}$ with $\alpha \neq \beta$.

Since the atoms and ions of the solar medium in which neutrinos propagate are non-relativistic, the vector part of the *nsi* operator gives the dominant contribution for the interactions of the neutrinos with the plasma of the Sun's interior, in which

case the effective nsi coupling can be described by the following combination [57]: $\epsilon_{\alpha\beta}^f = \epsilon_{\alpha\beta}^{fL} + \epsilon_{\alpha\beta}^{fR}$. These new kinds of neutrino interactions lead to a new effective potential difference to describe the propagation of neutrinos in matter [59]. Accordingly, the effective potential difference $V_{\alpha\beta}$ is written as a generalization of the $V_{\alpha\beta}$ obtained in the standard case: equations 11 and 13. Hence, $V_{\alpha\beta}$ reads

$$V_{\alpha\beta} = V_e \delta_{\alpha e} \delta_{\beta e} + \sqrt{2} G_F \sum_f \epsilon_{\alpha\beta}^f n_f(r) \quad (20)$$

where $\epsilon_{\alpha\beta}^f$ is the strength of nsi interaction of neutrinos with the medium. A more detailed discussion about the relations between $\epsilon_{\alpha\beta}^f$ and $\epsilon_{\alpha\beta}^{fP}$ can be found in Gonzalez-Garcia and Maltoni [57]. Usually, $\epsilon_{\alpha\beta}^f$ is considered as a free parameter to be adjusted to fit the solar observational data.

In this work, we study only the nsi interactions of electron neutrinos (ν_e) with the solar plasma. Accordingly, as is common practice, we chose to take into account only the nsi coupling of electron neutrinos with the up-quarks and down-quarks of the solar plasma. Among others, Friedland et al. [60] have shown that the coupling of electron neutrinos with up-quarks is parametrized by a set of two independent parameters ($\epsilon_N^u, \epsilon_D^u$), and similarly the coupling of electron neutrinos with down-quarks is parametrized by another set of two independent parameters ($\epsilon_N^d, \epsilon_D^d$). Each of these parameters corresponds to a linear combination of the original parameters $\epsilon_{\alpha\beta}^f$ which defines the strength of the non-standard neutrino interactions with fermions as defined in equation 19. In the appendix A we show the relation of ϵ_D^f and ϵ_N^f with the parameters $\epsilon_{\alpha\beta}^f$, for which f is either d or u since in our study we are only concerned about the interaction with down- and up-quarks of the solar plasma. A detailed account of the relevance of these quantities can be found in Gonzalez-Garcia and Maltoni [e.g., 57], Maltoni and Smirnov [e.g., 59], Friedland et al. [e.g., 60].

As in the case of standard neutrino interactions, for these nsi interactions the oscillations of neutrino flavour are still adiabatic, so the probability of electron neutrino survival is given by equation (14). However, in this case the quantity $\cos(2\theta_m)$ has been redefined to take into account the new effective matter potential [59], accordingly

$$\cos(2\theta_{12}^m) \approx - \frac{V_{nsi}^*}{\sqrt{V_{nsi}^{*2} + (2r_f \epsilon_N^f + A_{12}^{*-1} \sin(2\theta_{12}))^2}} \quad (21)$$

where V_{nsi}^* reads

$$V_{nsi}^*(E, r) = c_{13}^2 - A_{12}^{*-1} \cos(2\theta_{12}) - 2r_f \epsilon_D^f. \quad (22)$$

where $r_f(r) = n_f(r)/n_e(r)$. Figure 3 shows the variation of the ratios $r_u(r)$ and $r_d(r)$ inside the star. The $r_d(r)$ is smaller than $r_u(r)$ because the star's composition is dominated by free protons (ionized hydrogen). As such, for each down-quark there are two up-quarks.

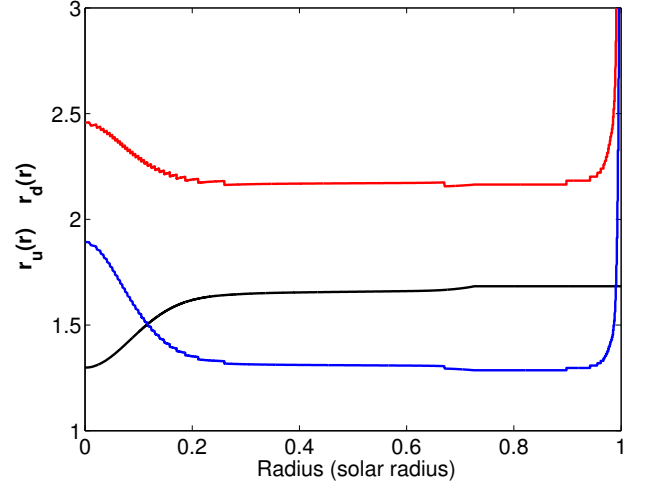


FIG. 3. Variation with the solar radius of the ratios $r_u(r) = n_u(r)/n_e(r)$ (red curve) and $r_d(r) = n_d(r)/n_e(r)$ (blue curve), and relative variation of up and down quarks $n_u(r)/n_d(r)$ (black curve).

F. The electron neutrino probability survival

The neutrino emission reactions of the pp chains and the CNO cycle are produced at high temperatures in distinct layers in the Sun's core. Similarly, the neutrino flavour oscillations occur in the same regions. The average survival probability of electron neutrinos in each nuclear reaction region is given by

$$\langle P_e(E) \rangle_j = N_j^{-1} \int_0^{R_\odot} P_e(E, r) \phi_j(r) 4\pi \rho(r) r^2 dr \quad (23)$$

where N_j is a normalization constant given by $N_j = \int_0^{R_\odot} \phi_j(r) 4\pi \rho(r) r^2 dr$ and $\phi_j(r)$ is the electron neutrino emission function for the j nuclear reaction. j corresponds to the following electron neutrino nuclear reactions: PP , PeP , 8B , 7Be , ${}^{13}N$, ${}^{15}O$ and ${}^{17}F$. $\phi_j(r)$ defines the location where neutrinos are produced in each nuclear reaction j for which the production is maximum in the layer of radius r_j (Cf. figure 1). The neutrino fluxes produced by the different nuclear reactions are sensitive to the local values of the temperature, molecular weight, density and electronic density. In this study, we consider that all neutrinos produced in the solar nuclear reactions are of electron flavour as predicted by standard nuclear physics, therefore, the local density of quarks only affects the $\langle P_e(E) \rangle_j$ by modifying the flavour of electron neutrinos by a new nsi interaction like the generalized MSW mechanism.

The survival probability of electron neutrinos $\langle P_e(E) \rangle_j$ given by equation (23) is computed using equations (14), (21) and (22). Figures 4 and 5 show $\langle P_e(E) \rangle_j$ for the different solar neutrino sources, either in the standard MSW or a generalized MSW. The different neutrino interaction models are described by a specific set of parameters: ($\epsilon_N^u, \epsilon_D^u, \epsilon_N^d, \epsilon_D^d$). Figures 4 and 5 top panels show $\langle P_e(E) \rangle_j$ for the standard MSW mechanism in which case all the parameters mentioned above are equal to zero. The other panels of Fig-

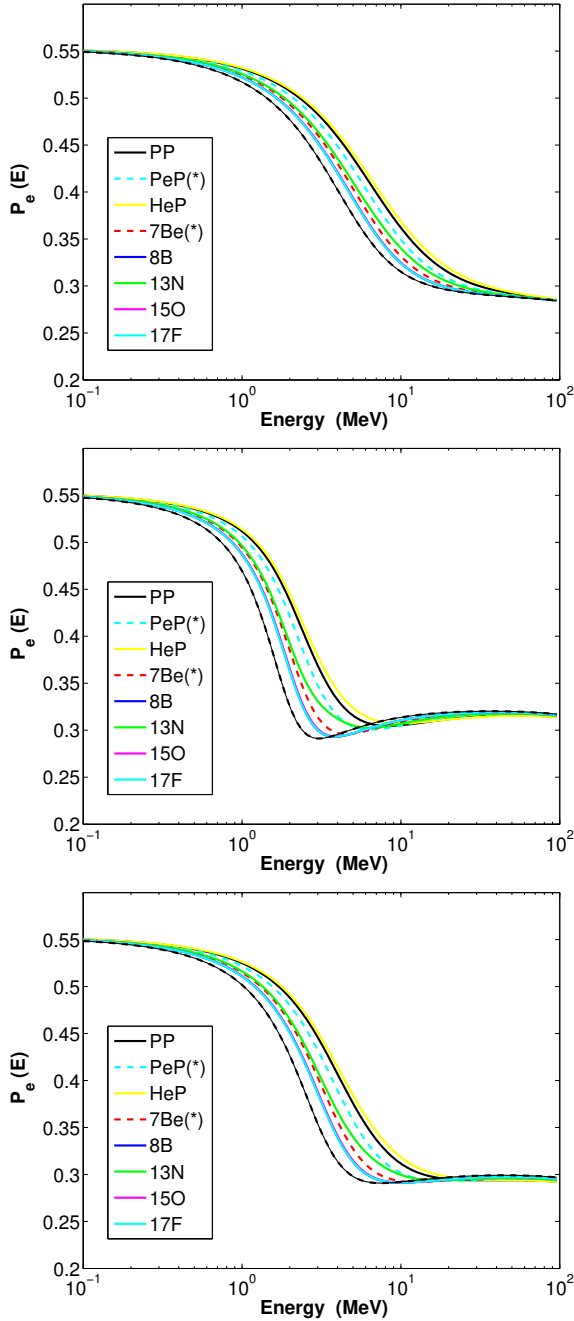


FIG. 4. The survival probability of electron-neutrinos: the P_e curves correspond to neutrinos produced in the nuclear reactions located at different solar radius. The three panels correspond to the following neutrino models of interaction: si -interaction with electrons (*top panel*), nsi -interaction with up-quarks with the coupling constants, $\epsilon_N^u = -0.30$ and $\epsilon_D^u = -0.22$ (*middle panel*), and nsi -interaction with down-quarks with coupling constant, $\epsilon_N^d = -0.16$ and $\epsilon_D^d = -0.12$ (*bottom panel*). The reference dotted-black curve defines the survival probability of electron-neutrinos in the centre of the Sun for which the si - or nsi -MSW flavour oscillation mechanism is maximum. The other coloured curves follow the same colour scheme shown in Figure 1.

ures 4 and 5 correspond to a generalized MSW mechanism

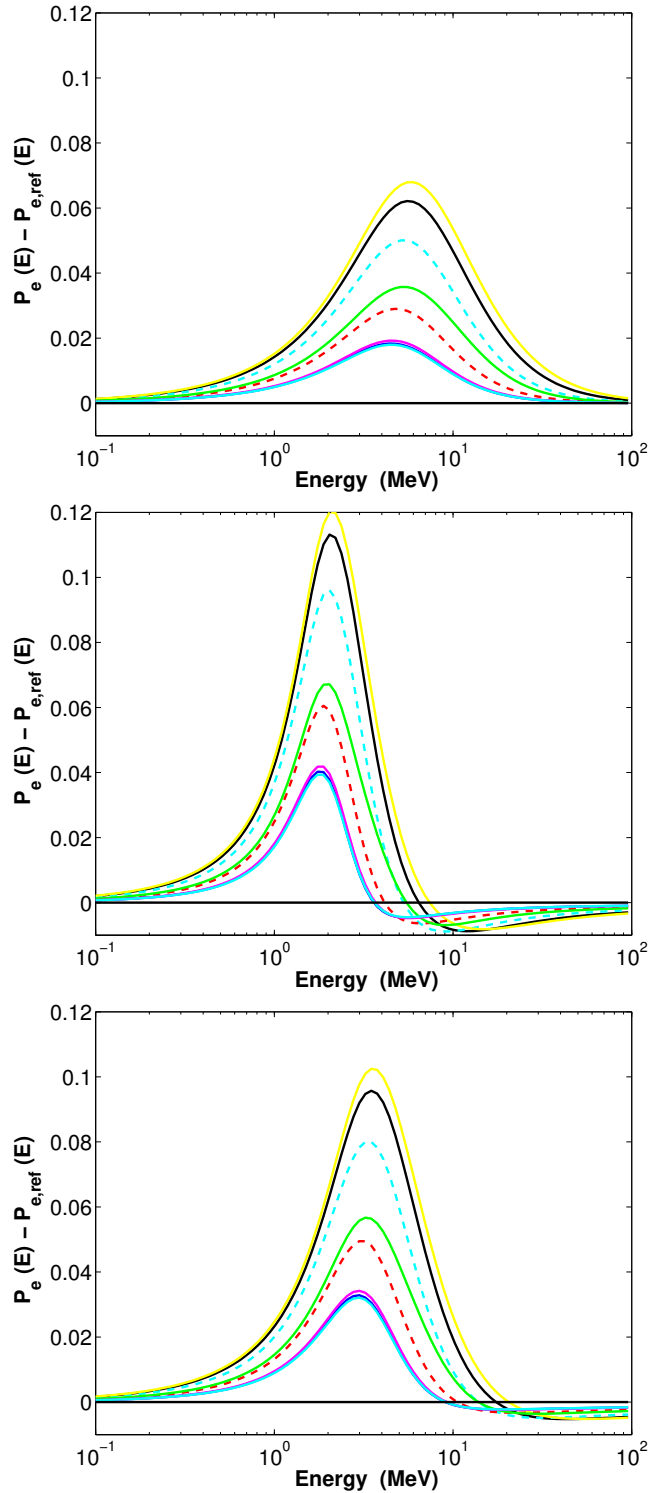


FIG. 5. The survival probability of electron-neutrinos in function of the neutrino energy for the different regions of emission. The different panels show the difference between the survival probability of the different electron neutrino sources and the reference curve (dotted-black curve in Figure 4). The coloured curves follow the same colour scheme shown in Figures 1 and 4.

for which the parameters ($\epsilon_N^u, \epsilon_D^u, \epsilon_N^d, \epsilon_D^d$) can have values

different of zero. Maltoni and Smirnov [59] among others have shown that only a relatively small ensemble of parameter combinations ($\epsilon_N^u, \epsilon_D^u, \epsilon_N^d, \epsilon_D^d$) can be accommodated with the current set of neutrino flux observations. In this study, for convenience, we choose to focus on neutrino interactions for which electron neutrinos couples either with up-quarks (for which $\epsilon_N^d = \epsilon_D^d = 0$) or with down-quarks (for which $\epsilon_N^u = \epsilon_D^u = 0$). Specifically, we chose two fiducial sets of values ($\epsilon_N^f, \epsilon_D^f, f = u, d$) of the ensemble of parameters that fits simultaneously the solar and KamLAND neutrino data sets with good accuracy. Figure 4 shows the survival probability of electron-neutrinos in the case of the *nsi*-interaction for the parameters sets: ($\epsilon_N^u = -0.30, \epsilon_D^u = -0.22$) and ($\epsilon_N^d = -0.16, \epsilon_D^d = -0.12$). As discussed by Maltoni and Smirnov [59] these values correspond to the two parameters that best fit simultaneously the current solar and KamLAND neutrino data sets. Figures 4 and 5 middle panels show $\langle P_e(E) \rangle_j$ for a neutrino up-quark interaction model, and Figures 4 and 5 bottom panels show $\langle P_e(E) \rangle_j$ for a neutrino down-quark interaction model.

All the different neutrino interaction models have several common features. In general the $\langle P_e(E) \rangle_j$ are very similar for low- and high-energy neutrinos. It is only for neutrinos with intermediate energy that it is possible to distinguish between the different models (Cf. figure 4). For neutrinos in this energy interval it is possible to distinguish two effects: one relates with the location of the different neutrino sources, and a second effect relates with the parameter values ($\epsilon_N^u, \epsilon_D^u, \epsilon_N^d, \epsilon_D^d$) of the neutrino interaction model. In the former effect, the $\langle P_e(E) \rangle_j$ differentiation results from the fact that $\phi_j(r)$ are located at different solar radius, as shown in figure 1. Such effect arises equally in *si*- and *nsi*- neutrino interaction models. The second effect occurs only for *nsi*-neutrino interaction models, and it is related with the radial distribution of up- and down-quarks (cf. Figure 2).

This latter effect is shown in figures 4 and 5 for the two fiducial models adopted in this study: a pure neutrino up-quark model ($\epsilon_N^d = \epsilon_D^d = 0$) and a pure neutrino down-quark model ($\epsilon_N^u = \epsilon_D^u = 0$). Accordingly, for neutrinos with an intermediate energy, the $\langle P_e(E) \rangle_j$ corresponding to the neutrino up-quark interaction model has an impact of larger amplitude than the neutrino down-quark interaction model (compare middle and bottom panels in figure 5). For instance, this effect is very significant for the $\langle P_e(E) \rangle_{pp}$. Nevertheless, these preliminary results should be interpreted with caution, since each neutrino source only produces neutrinos within a limited range of energy, as such the *nsi*-effect of $\langle P_e(E) \rangle_j$ shown in figure 5 can be significantly reduced in the final neutrino spectrum of some solar neutrino sources. Indeed, we remind that the neutrinos emitted by $\phi_j(r)$ are limited to a specific energy range for each j - nuclear reaction. As such only an energy portion of $\langle P_e(E) \rangle_j$ affects the final emitted neutrino spectrum. This point will be discussed in more detail in the next section.

IV. THE SOLAR ELECTRON NEUTRINO SPECTRA

The solar energy spectrum of electron neutrinos from any specific nuclear reaction is known to be essentially independent of solar parameters, that is, the energy spectrum created by a specific nuclear reaction is the same independently of whether neutrinos are produced in an Earth laboratory or in the core of the Sun. Therefore, the neutrino energy spectrum of the different nuclear reactions, can be assumed to be equivalent to its Earth laboratory counterpart. A typical example of such spectra is the ${}^8\text{B}$ neutrino energy spectrum emitted by the ${}^8\text{B}$ nuclear reaction of the *pp* chains in the Sun's core. This solar neutrino spectrum has been shown to be equivalent to several experimental determinations of the ${}^8\text{B}$ neutrino spectrum [e.g. 61, 62]. Bahcall and Holstein [63], Napolitano et al. [64], among others, have shown that the ${}^8\text{B}$ neutrino spectrum emitted in the Sun's core is equal to the spectrum measured in the laboratory, as the surrounding solar plasma does not affect this type of nuclear reaction. The ${}^8\text{B}$ neutrino spectrum measured in the laboratory agrees remarkably well with its theoretical prediction for neutrinos with an energy below 12 MeV, a small difference appearing only for high energy neutrinos. The experimental ${}^8\text{B}$ neutrino spectrum deduced from four laboratory experiments shows a difference with the theoretical prediction at most of 1% [62, 65–68]. Accordingly, we will consider that the electron neutrino energy spectrum of a solar nuclear reaction at the specific location where these neutrinos are created is identical to the equivalent neutrino spectrum measured in the laboratory.

All neutrinos produced in the Sun's nuclear reactions are of electron neutrino type. It is only during the propagation phase that these neutrinos vary their flavour between electron, τ and μ . Suitably, we define the original energy spectrum of electron neutrinos by $\Psi_e^s(E)$ and the end energy spectrum of neutrinos after the neutrino flavour oscillations by $\Psi_e^\circ(E)$. The first spectrum, which is identical to the neutrino spectrum obtained in an Earth's laboratory, relates to the neutrinos produced in nuclear reactions (see figure 1). The latter spectrum corresponds to neutrinos that have their flavour modified by the vacuum oscillations and the generalized MSW oscillation mechanism.

Conveniently, the neutrino spectra $\Psi_e^s(E)$ and $\Psi_e^\circ(E)$ associated to each of the different solar nuclear reactions of the *pp*-chain and CNO-cycle are labelled by a unique subscript j which can take one of these values: *PP*, *HeP*, ${}^8\text{B}$, ${}^{13}\text{N}$, ${}^{15}\text{O}$ and ${}^{17}\text{F}$. Hence, the two previous neutrino energy spectra have a simple relation, it reads

$$\Psi_{e,j}^\circ(E) = \langle P_e(E) \rangle_j \Psi_{e,j}^s(E), \quad (24)$$

where $\langle P_e(E) \rangle_j$ is the survival probability of an electron neutrino of energy E . Figure 6 shows the shape of several neutrino spectra $\Psi_{e,j}^\circ(E)$. The final neutrino energy spectrum $\Psi_{e,j}^\circ(E)$ is significantly different from the original spectrum $\Psi_{e,j}^s(E)$. Indeed, while $\Psi_{e,j}^s(E)$ depends only on the properties of the nuclear reaction, $\Psi_{e,j}^\circ(E)$ becomes distinct from $\Psi_{e,j}^s(E)$ due to the contribution of neutrino flavour oscillations. Specifically, the $\Psi_{e,j}^\circ(E)$ depends on the fundamen-

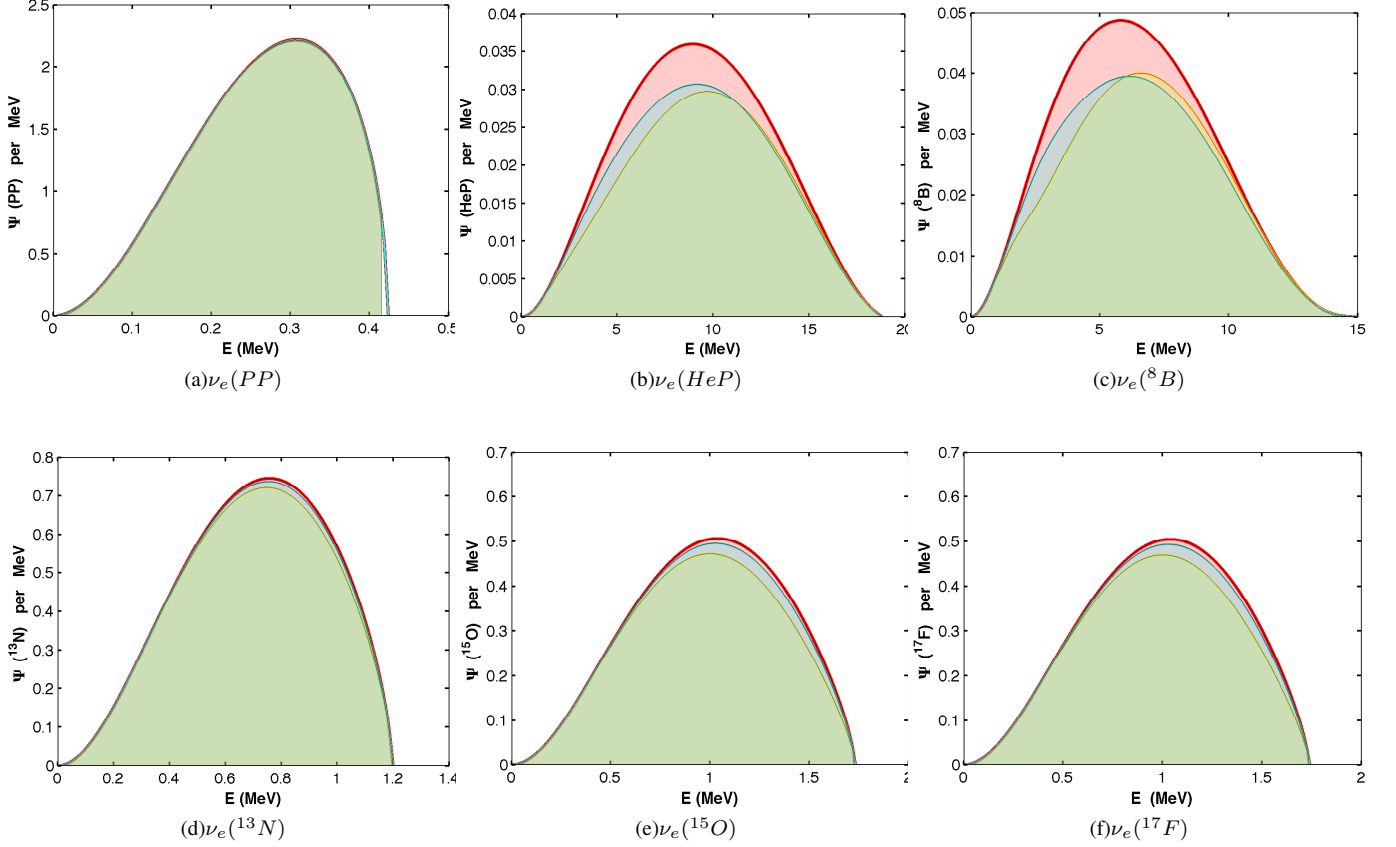


FIG. 6. pp -chain and cno -cycle energy neutrino spectra: $\Psi_{e,j}^{\odot}(E)$ is the electron solar neutrino spectrum for the standard MSW effect (red area); the other colour curves correspond to $\Psi_{e,j}^{e,j}(E)$, for which the generalized MSW effect is taken into consideration: nsi -neutrino interaction with up-quark (blue area), and nsi -neutrino interaction with down-quarks (green area). $\Psi_{e,j}^{\odot}(E)$ is defined as the probability per MeV of an electron-neutrino with an energy E . In the calculation of these neutrino spectra we used an up-to-date standard solar model.

tal parameters related with the neutrino vacuum oscillations through the (generalized) MSW oscillation mechanism, which depends on the local densities of electrons and quarks, and the nsi -coupling constants [69]. As discussed previously, all these effects are taken into account in $\langle P_e(E) \rangle_j$ (equation 23). In this study, we do not include the mono-energetic spectral lines of pp chains nuclear reactions PeP and 7Be . Although, the previous result (equation 24) also holds for these two neutrino sources (corresponds to the sources marked with the subscript $*$) in figure 1), we opt for not including them in this study, since for these neutrino sources other solar plasma properties contribute to change the shape of the neutrino spectral lines.

Figure 6 shows the spectra of electron neutrinos for some of the leading nuclear reactions of the Sun's core. The general shape of the spectra $\Psi_{e,j}^{\odot}(E)$ (equation 24) is a combination of the neutrino spectrum of the nuclear reaction $\Psi_{e,j}^{\odot}(E)$, and $\langle P_e(E) \rangle_j$ which depends of local density of electrons, down-quarks and up-quarks, as well as of the nsi -parameters of the generalized MSW mechanism. For the specific set of nsi -parameters discussed in this study, clearly the HeP and 8B neutrino emission shows the larger variation of the shape of

their spectra.

In both cases the interaction of neutrinos with (up- and down-) quarks leads to neutrino spectra with quite distinct shapes (blue and green areas in Figure 6) from the ones found in the standard MSW neutrino interaction (red area in Figure 6). Equally important is the fact that it is possible to distinguish between the two neutrino models of interaction with quarks, since each model depends differently of the neutrino energy. The ${}^{15}O$ and ${}^{17}F$ nuclear reactions also show neutrino spectra with different shapes, although in this case the impact of the nsi -interactions is much less pronounced than in the previous case, at least for the current set of parameters. For the two other nuclear reactions, PP and ${}^{13}N$, the impact of the nsi -interactions is very small. This is somehow expected since the energy of the neutrinos emitted in these nuclear reactions is relatively small. For this neutrino energy range the flavour oscillations are dominated by vacuum oscillations and are almost independent of matter oscillations.

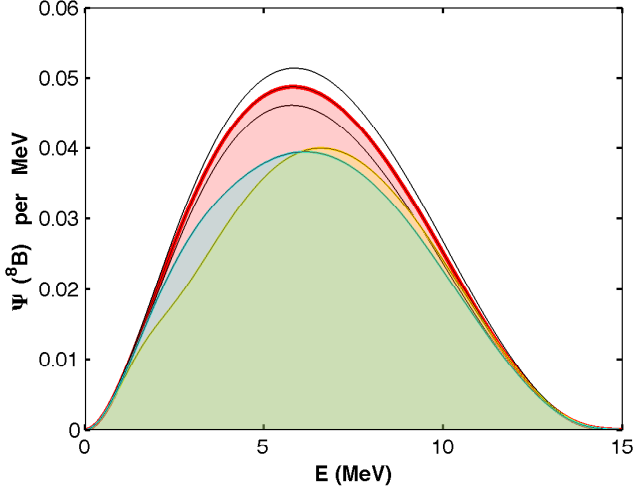


FIG. 7. The $\Psi_{e,8B}^{\odot}(E)$ is the electron solar neutrino spectrum for the standard MSW effect (red area) with the error bar computed for the forthcoming LENA experiment. The error (black lines) in the spectrum shape is computed assuming the error in the survival probability is $P_e(E) \pm 0.025$, which corresponds to 5 years of the LENA measurements. The coloured curves follow the same colour scheme shown in Figure 6. For clarity we have not included the error bar in the two other curves. Nevertheless, we note that the error bars for the other curves are identical to this one.

V. CONCLUSION

In this study we have computed the expected alteration in the shape of some leading solar neutrino spectra resulting from neutrinos having a new type of interactions with up- and down-quarks, identical to the MSW oscillations of neutrinos with electrons. This new type of matter interaction, also known as generalized MSW oscillations, depends of the specific properties of the neutrino interaction model but also of the local thermodynamic properties of the Sun's interior.

The study shows that the neutrino spectra of the different solar nuclear reactions have quite distinct sensitivities to the new neutrino physics. The HeP and $8B$ neutrino spectra have their shapes more affected by the new interaction between neutrinos and quarks. The $15O$ and $17F$ neutrino spectra also have a small alteration to their shapes, but these effects are much less pronounced than in the previous case. The impact of new physics in the PP and $13N$ spectra is also very small.

The new generation of neutrinos experiments such as Low Energy Neutrino Astronomy [LENA, 6], Jiangmen Underground Neutrino Observatory [JUNO, 7] Jinping Neutrino Experiment [Jinping, 10], Deep Underground Neutrino Experiment [DUNE, 8], and NO ν A Neutrino Experiment [NO ν A, 9], will allow to test some of new neutrino physics theories. The most promising evidence to discover $nsi-$ in solar neutrino data is the precise measurement of the $8B$ spectrum. Conveniently, we have estimated how the experimental error of the next generation of detectors like LENA [70] could affect our conclusion. In Figure 7 is show an error bar estima-

tion on the $8B$ spectrum computed assuming the error in the survival probability is $P_e(E) \pm 0.025$, which is the precision possible to be obtained for the electron neutrino survival probability after 5 years of LENA measurements [70]. Even in a relatively short period of 5 years of neutrino observations, it is already possible to find if neutrinos are experiencing flavour oscillations due to their interaction with quarks. Indeed, the identification by a future solar neutrino detector of a strong distortion in the shape of the solar neutrino spectrum, like the $8B$ neutrino spectrum compared to the one predicted by the standard solar model, will constitute a strong indication for the existence of interactions between neutrinos and quarks in the Sun's core. The location and magnitude of the distortion of the solar spectrum should give us some indication about the type of interaction (i.e., up- and down-quarks or both).

In conclusion, we have shown that in the near future neutrino spectroscopic measurements will be used to infer the new interaction between neutrinos and quarks. This will be an important and totally independent way of testing new neutrino physics interaction models.

ACKNOWLEDGMENTS

This work was supported by grants from Fundação para a Ciência e Tecnologia and Fundação Calouste Gulbenkian. The author thanks the anonymous referee for the comments and suggestions made to this work.

Appendix A: dimensionless parameters encoding the deviation from standard interactions

The interactions of neutrinos with matter in the theoretical framework of the non-standard model [e.g., 57] can be described by the Lagrangian term given by equation 19. In the following, it is assumed that electron neutrinos couples only with the up-quarks and down-quarks of the solar plasma (see section III E for details). For convenience, we adopt the parametrization of Gonzalez-Garcia and Maltoni [57], Maltoni and Smirnov [59], Friedland et al. [60] in which the coupling of electron neutrinos with either up-quarks or down-quarks of the solar plasma is parametrized by a set of two independent parameters $(\epsilon_N^u, \epsilon_D^u)$ or $(\epsilon_N^d, \epsilon_D^d)$. Accordingly, the coefficients ϵ_D^f and ϵ_N^f relate to the original parameters $\epsilon_{\alpha\beta}$ as

$$\begin{aligned} \epsilon_D^f &= c_{12}s_{13}Re \left[e^{i\delta_{CP}} (s_{23}\epsilon_{e\mu}^f + c_{23}\epsilon_{e\tau}^f) \right] \\ &\quad - (1 + s_{13}^2)c_{23}s_{23}Re(\epsilon_{\mu\tau}^f) \\ &\quad - \frac{c_{13}^2}{2}(\epsilon_{ee}^f - \epsilon_{\mu\mu}^f) + \frac{s_{23}^2 - s_{13}^2c_{23}^2}{2}(\epsilon_{\tau\tau}^f - \epsilon_{\mu\mu}^f) \end{aligned} \quad (A1)$$

and

$$\begin{aligned} \epsilon_N^f &= c_{13}(c_{23}\epsilon_{e\mu}^f - s_{23}\epsilon_{e\tau}^f) \\ &\quad + s_{13}e^{-i\delta_{CP}} \left[s_{23}\epsilon_{\mu\tau}^f - c_{23}^2\epsilon_{\mu\tau}^{f*} + c_{23}s_{23}(\epsilon_{\tau\tau}^f - \epsilon_{\mu\mu}^f) \right] \end{aligned} \quad (A2)$$

As in this work we are only interested in the interaction of neutrinos with the solar plasma, we will consider at a time the fol-

lowing values of f : e , u and d . A detailed discussion about the relevance of this parametrization can be found in Gonzalez-Garcia and Maltoni [e.g., 57], Friedland et al. [e.g., 60].

-
- [1] C. K. Jung, T. Kajita, T. Mann, and C. McGrew. Oscillations of Atmospheric Neutrinos. *Annual Review of Nuclear and Particle Science*, 51:451–488, 2001. doi: 10.1146/annurev.nucl.51.101701.132421.
- [2] T. Kajita and Y. Totsuka. Observation of atmospheric neutrinos. *Reviews of Modern Physics*, 73:85–118, January 2001. doi: 10.1103/RevModPhys.73.85.
- [3] Q. R. et al. Ahmad. Measurement of the Rate of Interactions $\nu_e + d \rightarrow p + p + e$ - Produced by ^8B Solar Neutrinos at the Sudbury Neutrino Observatory. *Physical Review Letters*, 87(7): 071301, August 2001. doi:10.1103/PhysRevLett.87.071301.
- [4] R. Davis, D. S. Harmer, and K. C. Hoffman. Search for Neutrinos from the Sun. *Physical Review Letters*, 20:1205–1209, May 1968. doi:10.1103/PhysRevLett.20.1205.
- [5] W. C. Haxton, R. G. Hamish Robertson, and A. M. Serenelli. Solar Neutrinos: Status and Prospects. *Annual Review of Astronomy and Astrophysics*, 51:21–61, August 2013. doi: 10.1146/annurev-astro-081811-125539.
- [6] M. et al. Wurm. The next-generation liquid-scintillator neutrino observatory LENA. *Astroparticle Physics*, 35:685–732, June 2012. doi:10.1016/j.astropartphys.2012.02.011.
- [7] F. et al. An. Neutrino physics with JUNO. *Journal of Physics G Nuclear Physics*, 43(3):030401, March 2016. doi: 10.1088/0954-3899/43/3/030401.
- [8] A. de Gouvêa and K. J. Kelly. Non-standard neutrino interactions at DUNE. *Nuclear Physics B*, 908:318–335, July 2016. doi:10.1016/j.nuclphysb.2016.03.013.
- [9] A. Friedland and I. M. Shoemaker. Searching for Novel Neutrino Interactions at NOvA and Beyond in Light of Large θ_{13} . *ArXiv e-prints:1207.6642*, July 2012.
- [10] J. F. et al. Beacom. Letter of Intent: Jinping Neutrino Experiment. *ArXiv e-prints:1602.01733*, February 2016.
- [11] A. et al. Bandyopadhyay. Physics at a future Neutrino Factory and super-beam facility. *Reports on Progress in Physics*, 72(10):106201, October 2009. doi:10.1088/0034-4885/72/10/106201.
- [12] A. et al. de Gouvea. Neutrinos. *ArXiv e-prints:1310.4340*, October 2013.
- [13] A. B. Balantekin and H. Yüksel. Physics potential of solar neutrino experiments. *Nuclear Physics B Proceedings Supplements*, 138:347–349, January 2005. doi: 10.1016/j.nuclphysbps.2004.11.080.
- [14] A. B. Balantekin, J. F. Beacom, and J. M. Fetter. Matter-enhanced neutrino oscillations in the quasi-adiabatic limit. *Physics Letters B*, 427:317–322, May 1998. doi: 10.1016/S0370-2693(98)00231-7.
- [15] I. Lopes. Search for Global f-Modes and p-Modes in the ^8B Neutrino Flux. *The Astrophysical Journal Letters*, 777:L7, November 2013. doi:10.1088/2041-8205/777/1/L7.
- [16] A. Serenelli, C. Peña-Garay, and W. C. Haxton. Using the standard solar model to constrain solar composition and nuclear reaction S factors. *Phys. Rev. D*, 87(4):043001, February 2013. doi:10.1103/PhysRevD.87.043001.
- [17] I. P. Lopes and J. Silk. Solar Neutrinos: Probing the Quasi-isothermal Solar Core Produced by Supersymmetric Dark Matter Particles. *Physical Review Letters*, 88(15):151303, April 2002. doi:10.1103/PhysRevLett.88.151303.
- [18] R. et al. Wendell. Atmospheric neutrino oscillation analysis with subleading effects in Super-Kamiokande I, II, and III. *Physical Review D*, 81(9):092004, May 2010. doi: 10.1103/PhysRevD.81.092004.
- [19] P. et al. Adamson. Electron Neutrino and Antineutrino Appearance in the Full MINOS Data Sample. *Physical Review Letters*, 110(17):171801, April 2013. doi: 10.1103/PhysRevLett.110.171801.
- [20] K. Abe, J. Adam, H. Aihara, T. Akiri, C. Andreopoulos, S. Aoki, A. Ariga, T. Ariga, S. Assylbekov, D. Autiero, and et al. Observation of Electron Neutrino Appearance in a Muon Neutrino Beam. *Physical Review Letters*, 112(6):061802, February 2014. doi:10.1103/PhysRevLett.112.061802.
- [21] O. G. Miranda and H. Nunokawa. Non standard neutrino interactions: current status and future prospects. *New Journal of Physics*, 17(9):095002, September 2015. doi:10.1088/1367-2630/17/9/095002.
- [22] T. Ohlsson. Status of non-standard neutrino interactions. *Reports on Progress in Physics*, 76(4):044201, April 2013. doi: 10.1088/0034-4885/76/4/044201.
- [23] I. Girardi, D. Meloni, and S. T. Petcov. The Daya Bay and T2K results on $\sin^2 \theta_{13}$ and non-standard neutrino interactions. *Nuclear Physics B*, 886:31–42, September 2014. doi: 10.1016/j.nuclphysb.2014.06.014.
- [24] S. Turck-Chieze and I. Lopes. Toward a unified classical model of the sun - On the sensitivity of neutrinos and helioseismology to the microscopic physics. *The Astrophysical Journal*, 408: 347–367, May 1993. doi:10.1086/172592.
- [25] P. Morel. CESAM: A code for stellar evolution calculations. *A & A Supplement series*, 124, 597, September 1997. doi: 10.1051/aas:1997209.
- [26] M. Asplund, N. Grevesse, and A. J. Sauval. The Solar Chemical Composition. In T. G. Barnes, III and F. N. Bash, editors, *Cosmic Abundances as Records of Stellar Evolution and Nucleosynthesis*, volume 336 of *Astronomical Society of the Pacific Conference Series*, San Francisco, page 25, September 2005.
- [27] M. Asplund, N. Grevesse, A. J. Sauval, and P. Scott. The Chemical Composition of the Sun. *Annual Review of Astronomy & Astrophysics*, 47:481–522, September 2009. doi: 10.1146/annurev.astro.46.060407.145222.
- [28] S. Turck-Chièze and S. Couvidat. Solar neutrinos, helioseismology and the solar internal dynamics. *Reports on Progress in Physics*, 74(8):086901, August 2011. doi:10.1088/0034-4885/74/8/086901.
- [29] S. Turck-Chièze, S. Couvidat, L. Piau, J. Ferguson, P. Lambert, J. Ballot, R. A. García, and P. Nghiem. Surprising Sun: A New Step Towards a Complete Picture? *Physical Review Letters*, 93(21):211102, November 2004. doi: 10.1103/PhysRevLett.93.211102.
- [30] J. N. Bahcall, S. Basu, M. Pinsonneault, and A. M. Serenelli. Helioseismological Implications of Recent Solar Abundance Determinations. *The Astrophysical Journal*, 618:1049–1056, January 2005. doi:10.1086/426070.
- [31] J. N. Bahcall, A. M. Serenelli, and S. Basu. New Solar Opacities, Abundances, Helioseismology, and Neutrino Fluxes.

- The Astrophysical Journal*, 621:L85–L88, March 2005. doi:10.1086/428929.
- [32] A. M. Serenelli, S. Basu, J. W. Ferguson, and M. Asplund. New Solar Composition: The Problem with Solar Models Revisited. *The Astrophysical Journal Letters*, 705:L123–L127, November 2009. doi:10.1088/0004-637X/705/2/L123.
- [33] J. A. Guzik and K. Mussack. Exploring Mass Loss, Low-Z Accretion, and Convective Overshoot in Solar Models to Mitigate the Solar Abundance Problem. *The Astrophysical Journal*, 713:1108–1119, April 2010. doi:10.1088/0004-637X/713/2/1108.
- [34] S. Turck-Chièze, A. Palacios, J. P. Marques, and P. A. P. Nghiem. Seismic and Dynamical Solar Models. I. The Impact of the Solar Rotation History on Neutrinos and Seismic Indicators. *The Astrophysical Journal*, 715:1539–1555, June 2010. doi:10.1088/0004-637X/715/2/1539.
- [35] S. Turck-Chièze and I. Lopes. Solar-stellar astrophysics and dark matter. *Research in Astronomy and Astrophysics*, 12:1107–1138, August 2012. doi:10.1088/1674-4527/12/8/011.
- [36] N. Grevesse and A. J. Sauval. Standard Solar Composition. *Space Science Reviews*, 85:161–174, May 1998. doi:10.1023/A:1005161325181.
- [37] S. Vagnozzi, K. Freese, and T. H. Zurbuchen. A successful solar model using new solar composition data. *ArXiv e-prints:1603.05960*, March 2016.
- [38] M. C. Gonzalez-Garcia and M. Maltoni. Phenomenology with massive neutrinos. *Physics Reports*, 460:1–129, April 2008. doi:10.1016/j.physrep.2007.12.004.
- [39] G. Bellini, L. Ludhova, G. Ranucci, and F. L. Villante. Neutrino oscillations. *Advances in High Energy Physics*, Volume 2014 (2014), Article ID 191960, doi:10.1155/2014/191960.
- [40] D. K. Papoulias and T. S. Kosmas. Standard and non-standard neutrino-nucleus reactions cross sections and event rates to neutrino detection experiments. *Advances in High Energy Physics*, Volume 2015 (2015), Article ID 763648, doi:10.1155/2015/763648.
- [41] S. Davidson, C. P. na-Garay, N. Rius, and A. Santamaria. Present and future bounds on non-standard neutrino interactions. *Journal of High Energy Physics*, 3:011, March 2003. doi:10.1088/1126-6708/2003/03/011.
- [42] T. W. Donnelly and J. D. Walecka. Semi-leptonic weak and electromagnetic interactions with nuclei: Isoelastic processes. *Nuclear Physics A*, 274:368–412, December 1976. doi:10.1016/0375-9474(76)90209-8.
- [43] D. Nötzold and G. Raffelt. Neutrino dispersion at finite temperature and density. *Nuclear Physics B*, 307:924–936, October 1988. doi:10.1016/0550-3213(88)90113-7.
- [44] K. A. Olive and Particle Data Group. Review of Particle Physics. *Chinese Physics C*, 38(9):090001, August 2014. doi:10.1088/1674-1137/38/9/090001.
- [45] C. Giunti and W. K. Chung. *Fundamentals of Neutrino Physics and Astrophysics*. Oxford University Press, 2007.
- [46] T. K. Kuo and J. Pantaleone. Neutrino oscillations in matter. *Reviews of Modern Physics*, 61:937–980, October 1989. doi:10.1103/RevModPhys.61.937.
- [47] K. Huitu, T. J. Kärkkäinen, J. Maalampi, and S. Vihonen. Constraining the nonstandard interaction parameters in long baseline neutrino experiments. *Phys. Rev. D*, 93(5):053016, March 2016. doi:10.1103/PhysRevD.93.053016.
- [48] J. Bergström, M. C. Gonzalez-Garcia, M. Maltoni, and T. Schwetz. Bayesian global analysis of neutrino oscillation data. *Journal of High Energy Physics*, 9:200, September 2015. doi:10.1007/JHEP09(2015)200.
- [49] M. C. Gonzalez-Garcia, M. Maltoni, and T. Schwetz. Updated fit to three neutrino mixing: status of leptonic CP violation. *Journal of High Energy Physics*, 11:52, November 2014. doi:10.1007/JHEP11(2014)052.
- [50] M. Apollonio and A. Baldini. Limits on neutrino oscillations from the CHOOZ experiment. *Physics Letters B*, 466:415–430, November 1999. doi:10.1016/S0370-2693(99)01072-2.
- [51] G. L. Fogli, E. Lisi, A. Marrone, A. Palazzo, and A. M. Rotunno. Neutrino oscillations, global analysis and theta(13). *ArXiv e-prints:0905.3549*, May 2009.
- [52] G. L. Fogli, E. Lisi, A. Marrone, D. Montanino, A. Palazzo, and A. M. Rotunno. Global analysis of neutrino masses, mixings, and phases: Entering the era of leptonic CP violation searches. *Physical Review D*, 86(1):013012, July 2012. doi:10.1103/PhysRevD.86.013012.
- [53] P. Hernandez. Neutrino physics. *ArXiv e-prints:1010.4131*, October 2010.
- [54] A. B. Balantekin and H. Yuksel. Global Analysis of Solar Neutrino and KamLAND Data. *ArXiv High Energy Physics - Phenomenology e-prints:hep-ph/0301072*, January 2003.
- [55] S. Goswami and A. Y. Smirnov. Solar neutrinos and 1-3 leptonic mixing. *Physical Review D*, 72(5):053011, September 2005. doi:10.1103/PhysRevD.72.053011.
- [56] M. Thomson. *Modern Particle Physics*. (Cambridge University Press. Cambridge, UK, 2013)
- [57] M. C. Gonzalez-Garcia and M. Maltoni. Determination of matter potential from global analysis of neutrino oscillation data. *Journal of High Energy Physics*, 9:152, September 2013. doi:10.1007/JHEP09(2013)152.
- [58] Y. Farzan. A model for large non-standard interactions of neutrinos leading to the LMA-Dark solution. *Physics Letters B*, 748:311–315, September 2015. doi:10.1016/j.physletb.2015.07.015.
- [59] M. Maltoni and A. Y. Smirnov. Solar neutrinos and neutrino physics. *European Physical Journal A*, 52:87, April 2016. doi:10.1140/epja/i2016-16087-0.
- [60] A. Friedland, C. Lunardini, and M. Maltoni. Atmospheric neutrinos as probes of neutrino-matter interactions. *Physical Review D*, 70(11):111301, December 2004. doi:10.1103/PhysRevD.70.111301.
- [61] C. E. Ortiz, A. García, R. A. Waltz, M. Bhattacharya, and A. K. Komives. Shape of the ^8B Alpha and Neutrino Spectra. *Physical Review Letters*, 85:2909–2912, October 2000. doi:10.1103/PhysRevLett.85.2909.
- [62] W. T. Winter, S. J. Freedman, K. E. Rehm, and J. P. Schiffer. The ^8B neutrino spectrum. *Physical Review C*, 73(2):025503, February 2006. doi:10.1103/PhysRevC.73.025503.
- [63] J. N. Bahcall and B. R. Holstein. Solar neutrinos from the decay of ^8B . *Physical Review C*, 33:2121–2127, June 1986. doi:10.1103/PhysRevC.33.2121.
- [64] J. Napolitano, S. J. Freedman, and J. Camp. Beta and neutrino spectra in the decay of ^8B . *Physical Review C*, 36:298–302, July 1987. doi:10.1103/PhysRevC.36.298.
- [65] W. T. Winter, S. J. Freedman, K. E. Rehm, I. Ahmad, J. P. Greene, A. Heinz, D. Henderson, R. V. Janssens, C. L. Jiang, E. F. Moore, G. Mukherjee, R. C. Pardo, T. Pennington, G. Savard, J. P. Schiffer, D. Seweryniak, G. Zinkann, and M. Paul. Determination of the ^8B Neutrino Spectrum. *Physical Review Letters*, 91(25):252501, December 2003. doi:10.1103/PhysRevLett.91.252501.
- [66] T. et al. Roger. Precise Determination of the Unperturbed B8 Neutrino Spectrum. *Physical Review Letters*, 108(16):162502, April 2012. doi:10.1103/PhysRevLett.108.162502.
- [67] M. Bhattacharya, E. G. Adelberger, and H. E. Swanson. Precise study of the final-state continua in Li8 and B8 decays. *Physical Review C*, 73(5):055802, May 2006. doi:

- 10.1103/PhysRevC.73.055802.
- [68] O. S. Kirsebom, S. Hyldegaard, M. Alcorta, M. J. G. Borge, J. Büscher, T. Eronen, S. Fox, B. R. Fulton, H. O. U. Fynbo, H. Hultgren, A. Jokinen, B. Jonson, A. Kankainen, P. Karvonen, T. Kessler, A. Laird, M. Madurga, I. Moore, G. Nyman, H. Penttilä, S. Rahaman, M. Reponen, K. Riisager, T. Roger, J. Ronkainen, A. Saastamoinen, O. Tengblad, and J. Äystö. Precise and accurate determination of the B8 decay spectrum. *Physical Review C*, 83(6):065802, June 2011. doi: 10.1103/PhysRevC.83.065802.
- [69] I. Lopes. Probing the Sun's inner core using solar neutrinos: A new diagnostic method. *Physical Review D*, 88(4):045006, August 2013. doi:10.1103/PhysRevD.88.045006.
- [70] R. Möllenberg, F. von Feilitzsch, D. Hellgartner, L. Oberauer, M. Tippmann, J. Winter, M. Wurm, and V. Zimmer. Detecting the upturn of the solar ^8B neutrino spectrum with LENA. *Physics Letters B*, 737:251–255, October 2014. doi: 10.1016/j.physletb.2014.08.053.